Published in final edited form as:
Neurochem Res. 2007 December ; 32(12): 2080–2093.

Mesenchymal stem cells from rat bone marrow down regulate Caspase-3 mediated apoptotic pathway after spinal cord injury in rats

Venkata Ramesh Dasari[1], **Daniel G. Spomar**[2], **Craig Cady**[3], **Meena Gujrati**[4], **Jasti S. Rao**[1,2], and **Dzung H. Dinh**[2]

1*Department of Cancer Biology and Pharmacology, University of Illinois College of Medicine, Peoria, IL 61656*

2*Department of Neurosurgery, University of Illinois College of Medicine at Peoria, Peoria, IL 61656*

3*Department of Biology, Bradley University, Peoria, IL 61625*

4*Department of Pathology, University of Illinois College of Medicine at Peoria, Peoria, IL 61656*

Abstract

Mesenchymal stem cells have been intensively studied for their potential use in reparative strategies for neurodegenerative diseases and traumatic injuries. We used mesenchymal stem cells (rMSC) from rat bone marrow to evaluate the therapeutic potential after spinal cord injury (SCI). Immunohistochemistry confirmed a large number of apoptotic neurons and oligodendrocytes in caudal segments 2mm away from the lesion site. Expression of caspase-3 on both neurons and oligodendrocytes after SCI was significantly downregulated by rMSC. Caspase-3 downregulation by rMSC involves increased expression of FLIP and XIAP in the cytosol and inhibition of PARP cleavage in the nucleus. Animals treated with rMSC had higher BBB scores and better recovery of hind limb sensitivity. Treatment with rMSC had a positive effect on behavioral outcome and histopathological assessment after SCI. The ability of rMSC to incorporate into the spinal cord, differentiate and to improve locomotor recovery hold promise for a potential cure after SCI.

Keywords

Rat bone marrow stem cells; Spinal cord injury; Apoptosis; Caspase-3; BBB scores; Functional recovery

Introduction

The use of stem cells as transplant tissue shows particular promise since they may serve as a bridge to support regeneration and also differentiate into neurons or glia, thereby replacing endogenous cells destroyed by injury (1,2). Multipotential stem cells in adult bone marrow can generate glial and neuronal-like cells with appropriate treatment in culture and can differentiate into astrocytes, oligodendrocyte-like cells, and cells expressing markers of immature neurons *in vivo*(1,3,4).

Spinal cord injury is a destructive neurologic injury resulting in functional deficits due to the loss of spinal cord neurons and axons. In recent years, much attention has been given to

Corresponding Author: Dzung H. Dinh, M.D., Department of Neurosurgery, University of Illinois College of Medicine at Peoria, One Illini Drive, Peoria, IL 61605, USA, (309) 655-2642 – phone; (309) 655-7696 - fax; e-mail: ddinh@uic.edu.

secondary injury since this appears to be susceptible for therapeutic intervention. A cascade of neurotoxic events signifies the secondary injury after primary insult in the spinal cord, which includes local inflammatory response and apoptosis. Early apoptosis of neural cells including neurons is followed by a delayed wave of predominantly oligodendroglial apoptosis in degenerating white matter tracts (5-9). Apoptosis in white matter after dorsal cordotomy or after transection suggest that glial apoptosis occurs, at least in part, as a consequence of axonal degeneration (10,11). Several studies have implicated the apoptotic role of caspases in the injured spinal cord (12-21). Fas expression, activation of caspases 3 and 8, and apoptosis occur in a temporally similar fashion after SCI (22). Since the natural capacity of the central nervous system to recover from injury is limited, current SCI research focuses on the use of regenerative potential of bone marrow-derived cells for the reduction of neuronal degeneration by replacing the damaged neurons and oligodendrocytes, by downregulating the apoptotic pathways especially by decreasing expression of Fas and caspases, or to achieve functional recovery through enhanced neuronal plasticity.

It is hypothesized that decreasing apoptosis in both oligodendrocytes and neurons by decreasing the expression of caspase-3 mediated apoptotic pathway may improve neurological outcome after SCI. Therefore, we used a combination of behavioral investigation and careful analysis of lesion histopathology to evaluate the effects of rMSC transplantation following spinal cord injury in rats. In the present study we cultivated a population of adherent non-hematopoietic bone marrow stromal cells, i.e. bone marrow mesenchymal stem cells (rMSC), which have been successfully differentiated into neurons, oligodendrocytes and astrocytes both *in vitro* and *in vivo* in the injured spinal cord. Further, we investigated whether rMSC could regulate caspase-3 mediated apoptotic pathway and thus improve functional recovery in rats after SCI.

Methods

Spinal cord injury of rat

Moderate spinal cord injury was induced using the weight drop device (NYU Impactor) as reported previously (8,15). Rats were assigned to different groups as described in Table 1. Briefly, adult male rats (Lewis; 250-300 g) were anesthetized with ketamine (100 mg/kg; ip) and xylazine (5 mg/kg; ip) (both from Med-Vet International, Mettawa, IL). A laminectomy was performed at the T9-T11 level exposing the cord beneath without disrupting the dura, and the exposed dorsal surface of the cord at T10 was subjected to a weight drop impact using a 10 g rod (2.5 mm in diameter) dropped at a height of 12.5 mm. After injury, the muscles and skin were closed in layers, and the rats were placed in a temperature and humidity-controlled chamber overnight. Cefazolin (25 mg/kg) (Fisher, Hanover Park, IL,) was given to prevent urinary tract infection for 3-7 days. Manual expression of the urinary bladder was performed two times per day until reflex bladder emptying was established. The Institutional Animal Care and Use Committee of the University of Illinois College of Medicine at Peoria approved all surgical interventions and post-operative animal care.

Behavioral assessment after SCI

A behavioral test was performed to measure the functional recovery of the rats' hind limbs following the procedure described in Basso *et al.* (23). The scale used for measuring hind limb function with these procedures ranges from a score of 0, indicating no spontaneous movement, to a maximum score of 21, with an increasing score indicating the use of individual joints, coordinated joint movement, coordinated limb movement, weight-bearing, and other functions. Rats were first gently adapted to the open field used for the test. After a rat had walked continuously in the open field, two investigators conducted 4-min testing sessions on each leg. Two individuals 'blinded' to rat treatment status performed the open-field test at least once a

week from day 1 post-SCI to 3 weeks post-laminectomy on all animals in the study. Behavioral outcomes and examples of specific BBB locomotor scores were recorded using digital video.

Narrow-beam crossing

This paradigm evaluates the ability of the rats to balance on 30 cm elevated wooden beams with a length of 1 m. Different beam shapes were used to increase the level of difficulty: two beams with rectangular cross-sections (2× 2 cm; 1.2 × 1.2 cm) and a beam with a round cross-section (2.5 cm in diameter) (24). Crossing one beam by properly placing both hindlimbs was scored as 2 points; a total of 1.5 points was assigned when an animal placed only one paw plantar on the beam. Only 1 point was given if the rat was able to cross the whole beam but was unable to place the hind paws, and 0.5 points was given if the rat could only traverse half of the beam. The score was zero in cases in which the rat was not able to cross at least half of the beam. The scores of all three beams were added to a maximum score of 6 points.

Culture and *in vitro* differentiation of stem cells

Rat primary mesenchymal stem cells isolated from the bone marrow of adult female Fisher 344 rats with markers integrin $\beta1^+$ and $CD54^+$ were obtained from Chemicon (Temecula, CA) and maintained per manufacturer's instructions in DMEM-low glucose (Invitrogen, Carlsbad, CA), supplemented with 10% heat-inactivated FBS (Hyclone, Logan, UT), 2 mM L-Glutamine and 1% solution of Penicillin and Streptomycin (Invitrogen, Carlsbad, CA). When cells reached 70% to 80% confluency, the cells were detached with TrypLE Express (Invitrogen, Carlsbad, CA) and centrifuged at 250 *g* for 3 minutes and replated and maintained at 37°C in an incubator with a 5% CO_2 atmosphere. An acclimatization step was carried out 24 h prior to neural induction by replacing the growth medium with preinduction medium consisting of Neurobasal A medium (Invitrogen, Carlsbad, CA) supplemented with 10% FBS (Hyclone, Logan, UT), 1% Penicillin-Streptomycin (Invitrogen, Carlsbad, CA), 1% 200 mM L-Glutamine (Mediatech Inc.-Fisher, Hanover Park, IL), 2% B27 (Invitrogen, Carlsbad, CA), 1% N2 (Invitrogen, Carlsbad, CA), bFGF (10 ng/mL, Invitrogen, Carlsbad, CA), β-NGF (10 ng/mL, Sigma, St. Louis, MO), BDNF (10 ng/mL, EMD Biosciences, San Diego, CA), and NT-3 (10 ng/mL, EMD Biosciences, San Diego, CA). Neural differentiation was then initiated the following day by incubating the cells in neurogenic medium [preinduction medium with 0.5 μM retinoid acid (Sigma, St. Louis, MO) and hEGF (10 ng/mL, Sigma, St. Louis, MO)]. The cells were then observed for differentiation from 6 to 10 days.

Intraspinal grafting of stem cells

BBB locomotor rating scores were obtained before transplantation of stem cells and every week after SCI. Animals were re-anesthetized as described above, and the laminectomy site was re-exposed. Sham control group animals were injected 7 days after laminectomy with 5 μL of sterile PBS using a 10 μL Hamilton syringe. The rMSC-treated group was injected 7 days after injury, with 5 μL mononuclear cell layer of rMSC (5×10^5 cells/μL) diluted in sterile PBS into the contusion site. These cells were delivered at a rate of 0.5 μL/min using a 10 μL Hamilton syringe. Thus, a total of 2.5×10^6 cells were grafted into each injured spinal cord.

Immunocytochemistry

Cultured rMSC were characterized with antibodies against neural and astroglial markers. For this, cultured cells were plated in Petri dishes and rinsed twice with PBS, then fixed in 4% paraformaldehyde. After additional PBS rinses, cells were blocked with 0.1 M PBS with 1% BSA for 1 h. Primary antibodies specific for neurons, oligodendrocytes, and astrocytes were used to label the plated cells. Primary antibodies (1:100 dilution) specific for stem cells mouse anti-integrin β1 (BD Biosciences, Franklin Lakes, NJ) or rabbit anti-integrin β1 (Chemicon, Temecula, CA)], for neurons rabbit anti-NF200 (Chemicon, Temecula, CA), for

oligodendrocytes [(mouse anti-CNPase (Abcam, Cambridge, MA) and for astrocytes [rabbit anti-GFAP (Abcam, Cambridge, MA)] were diluted in 0.1 M PBS containing 1% BSA and applied overnight at 4°C. Appropriate fluorescence-tagged goat anti-mouse or anti-rabbit secondary antibodies were diluted 1:200 in 0.1 M PBS containing 1% BSA and applied individually for 1 to 2 h at room temperature. The cells were observed using a fluorescence microscope (Olympus IX71, Olympus, Melville, NY) and a confocal microscope (Olympus Fluoview, Olympus, Melville, NY) and photographed.

Immunohistochemistry and colocalization studies

At 3 weeks or 6 weeks post injury, rats were deeply anesthetized with ketamine/xylazine and intracardially perfused with 4% paraformaldehyde in 0.1 M phosphate buffer (pH 7.4). The spinal cord was removed and fixed for 2 h. Serial sections (5 μm) were made from a 2 mm length of spinal cord centered on the injury epicenter. Representative sections were stained with hematoxylin and eosin and Luxol fast blue to assess tissue morphology and determine the injury epicenter. Serial sections (1 section every 200 μm) obtained from 1 and 2 mm of tissue rostral and caudal to the epicenter were used for immunohistochemical analysis of apoptosis by *in situ* TUNEL or activated caspase-3-mediated apoptotic proteins.

For *in vivo* differentiation, neuronal or glial markers were detected using fluorescent staining. We used the following primary antibodies: mouse anti-integrin β1 (BD Biosciences, Franklin Lakes, NJ) or rabbit anti-integrin β1 (Chemicon, Temecula, CA), rabbit anti-GFAP (Dako, Carpinteria, CA), rabbit anti-NF200 (Chemicon, Temecula, CA), and mouse anti-APC (EMD Biosciences, San Diego, CA). Rabbit anti-Caspase 8 (Biovision, Mountain View, CA), rabbit anti-Caspase-3 (Cell Signaling Technology Inc., Beverly, MA) and rabbit anti-Caspase 10 (Cell Signaling Technology Inc., Beverly, MA) were used for immunostaining of caspases. After staining with primary antibodies (1:100 dilution), the sections were washed three times in PBS (10 min/wash) and incubated in goat anti-mouse or anti-rabbit HRP-conjugated secondary antibodies (1:200 dilution). After 1 h, sections were washed three times in PBS (10 min/wash), and incubated in DAB solution (Sigma, St. Louis, MO) until staining was evident microscopically. For immunofluorescence studies, the sections were washed three times in PBS (10 min/wash) and incubated in Texas Red conjugated anti-mouse secondary antibody or FITC-conjugated anti-rabbit secondary antibody (all at 1:200 dilution) for 1 h at room temperature. Sections were then washed three times in PBS (10 min/wash), counter stained with DAPI and cover slipped using fluorescent mounting medium (Dako, Carpinteria, CA), and observed using both a fluorescence microscope (Olympus IX71, Olympus, Melville, NY) and a confocal microscope (Olympus Fluoview, Olympus, Melville, NY). Negative controls (without primary antibody or using isotype specific IgG) were maintained for all the samples. Sections in which polymerase was omitted were used as negative control (for TUNEL).

Cell counting

All morphological analyses were performed with tissue identified by animal number. Sections representing 1 and 2 mm of tissue from the injury epicenter of animals at 21 DPI and controls were used to quantify immunoreactive cells. Cell counting was carried out in 10 sections (5 rostral and 5 caudal to the injury epicenter) per segment per animal in a 1 mm^2 area of the lateral and dorsal white matter, and dorsal grey matter using Image-Pro Discovery software (Media Cybernetics, Silver Spring, MD). Apoptotic cells in the white and grey matter regions were counted in three randomly chosen sections per 1 mm length of spinal cord, and the numbers were averaged. These regions were chosen because of the spared tissue even after SCI.

Subcellular fractionation and Western blot analysis

Different protein levels in spinal cord tissue at 3 weeks after SCI were compared with those in laminectomy controls and treated samples. For Western blot analysis, rats were euthanized, and 5 mm lengths of spinal cord centered on T10 (the injury site) were rapidly removed, weighed, and frozen at -70°C until necessary for further experimentation. The tissues were resuspended in 0.2 mL of homogenization buffer pH 7.4 [250 mM sucrose, 10 mM HEPES, 10 mM Tris-HCl, 10 mM KCl, 1% NP-40, 1 mM NaF, 1 mM Na_3VO_4, 1 mM EDTA, 1 mM DTT, 0.5 mM PMSF plus protease inhibitors: 1 μg/mL pepstatin, 10 μg /mL leupeptin and 10 μg/mL aprotinin] and homogenized in a Dounce homogenizer. Tissue homogenate was centrifuged at 20,000 × *g* for 15 min at 4°C and the protein levels in the supernatant were determined using the BCA assay (Pierce, Rockford, IL). Samples (40 μg of total protein per well) were subjected to 10%-14% SDS-PAGE (25) and transferred onto nitrocellulose filters, and the reaction was detected with Hyperfilm-MP autoradiography film (Amersham, Piscataway, NJ). For Western blot analysis, the following antibodies were used: mouse anti-Fas (1:5000; BD Biosciences, Franklin Lakes, NJ), rabbit anti-Caspase 8 (1:500; Biovision, Mountain View, CA), rabbit anti-Caspase-3 (1:1000; Cell Signaling Technology Inc., Beverly, MA), rabbit anti-Caspase 10 (1:1000; Cell Signaling Technology Inc., Beverly, MA), rabbit anti-PARP (1:1000; Cell Signaling Technology Inc., Beverly, MA), rabbit anti-XIAP (1:1000; Cell Signaling Technology Inc., Beverly, MA) and mouse anti-GAPDH (1:1000; Novus Biologicals, Littleton, CO). The membranes were blocked with 5% nonfat skim milk in TBS for 1 h at room temperature and then incubated with primary antibodies overnight at 4°C. The membranes were then processed with HRP-conjugated secondary antibodies. Immunoreactive bands were visualized using chemiluminescence ECL Western blotting detection reagents (Amersham, Piscataway, NJ). Experiments were performed in triplicate to ensure reproducibility. Values for injured, treated and control samples (n > 3 each group) were compared using the Student's *t* test. A *p* value of <0.05 was considered significant.

In situ terminal-deoxy-transferase mediated dUTP nick end labeling (TUNEL) assay

A TUNEL apoptosis detection kit (Upstate Biotechnology Inc, Lake Placid, NY) was used for DNA fragmentation fluorescence staining according to the manufacturer's protocol. Briefly, injured, treated and sham control rats (n = 4) were perfusion-fixed with 4% paraformaldehyde 0.1 M phosphate buffer (pH 7.4). Serial 5 μm paraffin spinal cord sections at 500 μm intervals were stained with hematoxylin, eosin and Luxol Fast Blue to identify the injury epicenter. Tissue sections at the injury epicenter and at 1000 μm, 1500 μm and 2000 μm rostral and caudal were incubated for 60 min with a reaction mix containing biotin-dUTP and terminal deoxynucleotidyl transferase. Fluorescein-conjugated avidin was applied to the sample, which was then incubated in the dark for 30 min. Positively stained fluorescein-labeled cells were visualized and photographed by fluorescence microscopy. TUNEL-positive nuclei were counted through the white and grey matter regions of each section.

Determination of caspase-3 activity

Caspase-3 activity of tissue samples was measured using Caspase-3 assay kit (Sigma, St. Louis, MO). The Caspase-3 colorimetric assay is based on the hydrolysis of acetyl-Asp-Glu-Val-Asp p-nitroanilide (Ac-DEVD-pNA) by caspase-3, resulting in the release of the p-nitroaniline (pNA) moiety. p-Nitroaniline is detected at 405 nm (ε_{mM}=10.5). The concentration of the pNA released from the substrate is calculated from either the absorbance values at 405 nm or from a calibration curve prepared with pNA standards. Tissues between 1 and 2 mm from the injury epicenter were homogenized in 1X lysis buffer (250 mM HEPES, pH 7.4, 25 mM CHAPS, 25 mM DTT). Tissue homogenates were centrifuged at 20,000× g for 15 minutes at 4°C in a microcentrifuge, and the supernatant was used for the measurement of caspase-3 activity using a 96-well plate micro assay method. In a final volume of 100 μl, supernatant (= 50μg) of each

test sample was incubated for 30 min at room temperature in the working solution containing synthetic caspase-3 substrate, Ac-DEVD-AMC. The absorbance was read at 405 nm in an ELISA plate reader for a period of 30 min. Ac-DEVD-CHO inhibitor was used for inhibitor studies. Caspase-3 activity was calculated using a *p*-nitroaniline calibration curve, as micromolar per gram of wet tissue. The data is plotted as A_{405} versus time for each sample and activity is calculated as pmol/min.

Statistical analysis

Quantitative data from cell counts, Western blot analysis, and open field locomotor scores were evaluated for statistical significance by one-way ANOVA with replications. Data for each group were represented as mean ± SEM and compared with other groups for significance by one-way Analysis of Variance (ANOVA) followed by Bonferroni's post hoc test (multiple comparison tests) using a statistical software package—Graph Pad Prism version 3.02. Results were considered statistically significant at $p < 0.05$.

Results

In vitro differentiation of rMSC to neural phenotypes

To establish the trans-differentiation potential of rMSC to neural lineages before intraspinal grafting, we used double immunofluorescence techniques under *in vitro* conditions. Rat mesenchymal stem cells can be induced to differentiate and express neural-specific antigens in neurogenic medium. When exposed to hEGF/RA, rMSC morphologically appear to take on some of the features of neural cells in culture, such as long bipolar extensions and branching ends. After neural culture, cells from rMSC expressed the neural antigens found in neurons (NF200) (Fig. 1A), oligodendrocytes (CNPase) (Fig. 1B) and astrocytes (GFAP) (Fig. 1C). Complete neural differentiation was observed after 5 days in culture for rMSC in culture (Figs. 1D and 1E). After differentiation, these cells were maintained up to 30 days to avoid any artifacts. These results were further confirmed by western blot analysis using both undifferentiated and differentiated rMSC (Fig. 1F). For comparison of neural proteins, we used rat whole brain extract as positive control. Differentiated rMSC show significant amounts of NF-200 (neural marker) and CNPase (oligodendrocyte marker), as confirmed by quantitative analysis (Fig. 1G). About 70%-75% of rMSC showed trans-differentiation to neural phenotypes. Of the total differentiated population of rMSC, cells expressing neural marker, NF-200 constituted the major proportion (44.20%) followed by oligodendrocyte marker, CNPase (32.47%) and astrocytic marker, GFAP (23.33%). The rMSC expressed these markers only after culture in the neurogenic differentiation media.

Survival and *in vivo* differentiation of rMSC in the injured spinal cord

Further, we addressed the survival and trans-differentiation of rMSC *in vivo* in the injured spinal cord. Two weeks after transplantation, robust survival of transplanted rMSC was observed in the spinal cords of treated rats, with cells distributed around the cavities throughout the injury site. The highest density of rMSC was at the area of primary injury, and was gradually reduced as the border with intact spinal cord tissue was approached. No rMSC cells were found in areas of intact spinal cord. No similarly fluorescent cells were found in SCI only animals (injured group). The transplanted cells migrated up to 2 mm rostrocaudally in the white matter. The differentiation of these rMSC into several neural phenotypes in the injured spinal cord was traced by immunofluorescence studies. Surviving stem cells labeled with antibodies against markers specific for rMSC (integrin β1) could be visualized up to 5 weeks after intra spinal grafting. In treated rats, co-localization of rMSC with neurons (stained by NF-200) (Fig. 2A), oligodendrocytes (stained by mature oligodendrocyte marker APC) (Fig. 2B) and astrocytes (stained by GFAP) (Fig. 2C) significantly establishes the differentiation of these stem cells to specific neural phenotypes. Of the total differentiated stem cells *in vivo*, most surviving rMSC

were oligodendrocytes (52.82%) and neurons (28.36%), with some rMSC-derived astrocytes (18.82% were GFAP-labeled). In the rMSC treated group, rMSC-differentiated neurons, astrocytes and oligodendrocytes were observed up to 5 weeks in the dorsal region of the injury epicenter, up to 2 mm rostrocaudally.

Cellular apoptosis after SCI is reduced by rMSC

We hypothesized that rMSC must reduce apoptosis within a few weeks in order to restore neurological functions. As a prelude to investigations on caspase-3 activation, we first confirmed the occurrence of apoptosis in the spinal cord after SCI using Hoechst 33343 nuclear staining and the TUNEL method (Fig.3). Since we observed the differentiation of stem cells up to 2mm of the injury epicenter, we confined our study to this region rostrocaudally. Nuclear staining with Hoechst 33343 identified the presence of apoptotic cells in the injured spinal cord tissue (Fig. 3A). Quantitative estimation of apoptotic cells indicates that sham control rats had an average of 6 ± 1 apoptotic cells per mm^2 section regardless of whether the section was at 1 or 2 mm rostral or caudal to T10. In SCI rats, the number of apoptotic cells increased up to 40 ± 2, within the dorsal white matter, especially around the lesion epicenter. Notably, we observed significant reduction in the number of apoptotic cells in rMSC-treated sections (13 ± 1) (Fig. 3B). Spinal cord sections from injured and treated groups were analyzed for TUNEL-positive cells. Sham control rats showed an average of 3 ± 1 TUNEL-positive cells per mm^2 section regardless of whether the section was at 1 or 2 mm rostral or caudal to T10. In contrast, in SCI rats, there was an increase in TUNEL-positive cells to an average of 31 ± 1 within the dorsal white matter, especially around the lesion epicenter, accompanied by tissue loss. However, in rMSC- treated sections TUNEL positive cells showed significant reduction (6 ± 1) (Fig. 3B).

Subsequently, we focused the analysis of TUNEL positive cells in a 1 mm^2 area of the sections taken at 1 and 2 mm caudal to the epicenter. Comparison of TUNEL counts showed much difference between injured and treated rats at 21 days. Injured spinal cord tissues showed higher numbers of TUNEL-positive cells in the vicinity of 1 and 2 mm from the injury epicenter, which upon treatment with stem cells decreased significantly (Fig. 4). When compared to rostral region, caudal region showed higher numbers of TUNEL-positive cells. Similarly, higher numbers of TUNEL-positive cells were observed in the dorsal surface as compared to lateral surface. Based on these results, we confined our study to the dorsal surface of caudal region to the injury epicenter.

Down-regulation of caspase-3 activated extrinsic pathway by rMSC

Further, we decided to examine whether rMSC would decrease caspase-3 activation in the treated rats, by analyzing caspase-3 mediated extrinsic pathway in injured and rMSC-treated groups. In order to ascertain the activation of caspases during apoptosis after SCI, we examined the expression of caspases-3, -8 and -10 in tissue sections using immunostaining and Western blotting for activated caspases. We found greater activation of these caspases in injured sections when compared to sham control and stem cell-treated sections (Fig. 5) suggesting that less activation of caspase enzymes occurs in rMSC -treated rats after SCI.

Increased activity of the caspase family of proteases is associated with apoptosis, and it has been reported that caspase-3 plays a crucial role in SCI-mediated apoptotic cell death in the white matter (13,20). To ascertain the activation of caspase-3 during apoptosis after SCI, both injured and rMSC-treated samples were analyzed. Immunohistochemical analysis of spinal cord sections revealed the presence of active caspase-3 in injured sections not only at the lesion epicenter, but also distributed in the grey matter up to two segments away from the site of impact. We analyzed the number of caspase-3-positive cells in the white matter in 1 mm^2 areas. In SCI rats, caspase-3 positive cells are present at an average of 27 ± 1 which is more than two-fold compared to rMSC-treated rats (10 ± 1) (Fig. 6A). In SCI animals, the rostral portion

contained a lower number of caspase-3 positive cells than the caudal portion (data not shown). This is consistent with previous studies, which have reported that cells caudal to the injury epicenter exhibit more apoptosis as compared to the cells rostral to the epicenter (13).

Further, activity of caspase-3 enzyme in the tissues shows higher activity in the injured lysates compared to rMSC-treated tissues (Fig. 6B). In rMSC-treated rats, this activity is almost comparable to that of sham control uninjured rats, which confirms that some repair mechanisms are implicated by the rMSC. To understand the molecular mechanism of caspase-3 downregulation by rMSC, caspase-3-mediated apoptotic pathway proteins were analyzed by Western blot analysis (Fig. 7). Increase in the death ligand Fas was observed in the injured tissues as compared to rMSC treated tissues (Figs. 7A and 7B). The activation of Fas in the injured tissues triggered the activation of caspases-8, -10 and -3, which were efficiently downregulated by rMSC. On the other hand, in rMSC treatments upregulation of FLIP and XIAP was observed (Figs. 7C and 7D); these proteins are believed to serve as checkpoints of the apoptotic pathway in the cytosol. At the nuclear level, rMSC inhibited the cleavage of PARP. These data provide strong evidence that caspase-3 is implicated in the apoptotic cascade after SCI, and that rMSC probably inhibit apoptosis either by increasing the expression of FLIP and XIAP at the cytosolic level or by inhibiting the breakdown of PARP at the level of nucleus. Increase in caspase-3 and related apoptotic pathway proteins' expression, the caspase-3 enzymatic assay results, and the nicking of chromatin support the occurrence of Fastriggered caspase-3 activated apoptosis after traumatic SCI, which was efficiently downregulated by rMSC treatments.

In order to demonstrate the type of neuronal cells participating in the process of apoptosis, co-localization experiments were performed using caspase-3 with APC and NF-200 antibodies. Caspase-3 activity was found in both neurons and oligodendrocytes (Fig. 8). The presence of higher number of caspase-3-positive neurons (Figs. 8A and 8C) and oligodendrocytes (Fig. 8B and 8D) in injured sections establishes the role of caspase-3 on oligodendrocyte and neurons after SCI, which showed a decreasing trend in rMSC-treated sections. Quantitation of the number of caspase-3-positive neurons and oligodendrocytes (Fig. 8E) indicated that oligodendrocytes comprise a major population of the cells that undergo caspase-3 mediated apoptosis. However, in stem cell treatments, there was significant reduction in the number of apoptotic cells. Twenty-one days after injury, caspase-3-positive cells were observed at both 1 and 2 mm regions supporting previous results that SCI activates a caspase-3-dependent apoptotic pathway in glial cells (13,19).

Recovery of locomotor function by rMSC

BBB Scoring—Finally, we tested whether inhibition of apoptotic pathway proteins by rMSC can be correlated with the functional recovery of rats. The effect of rMSC on recovery of locomotor function after SCI was evaluated according to 21-point locomotor BBB scale, which is widely used (23). All injured rats receiving the experimental treatments exhibited a severe locomotion deficit one day after surgery (Fig. 9A). The mean BBB score in the injured group was 5.04±0.2 compared to 4.23 ± 0.5 in the rMSC-treated group before transplantation (7 days after SCI). Recovery of function improved slowly but steadily over the course of the three-week observation period in the rMSC -treated group. Rats in the transplanted group showed a significant improvement in the BBB scale relative to the injured group. For instance, after 14 days post-transplantation, some rMSC -treated rats were able to support their weight on the dorsal part of the paws while stationary or stepping, and others exhibited frequent to consistent steps with or without coordination (average BBB score of 12.95 ± 0.15). In contrast, injured rats only displayed movement of all three joints with occasional plantar placement, corresponding to an average BBB score of 9.65 ± 0.21. Our results further indicate that the improved recovery of function in the transplanted group was exclusive to the beneficial effects

of rMSC transplantation, because there was no significant difference in the performance of the injured group.

Narrow-beam crossing—This test reflects the capability of the animals to maintain balance while walking on beams with increasing degrees of difficulty (smaller diameter, round vs square). Before injury, all of the animals could cross the three differently shaped beams without any balancing difficulties (6 points) (Fig. 9B). Seven days after the injury, the average narrow-beam score of the injured rats was severely reduced from 6 to 0.32 ± 0.05 points, indicating that most rats lost balance as soon as they were placed on the beams. After one week of rMSC transplantation, treated rats showed an average score of 1.25 ± 0.12, reflecting their ability to cross the whole length of the broadest beam. Over the next week, the performance in this test recovered modestly, so that 14d after the rMSC grafting, the average narrow-beam score of the injured group was 0.82 ± 0.17 and that of the rMSC-treated was 1.62 ± 0.21. One rMSC-treated rat was able to cross all three beams. Statistically, rMSC treatment led to a significant improvement 14 d after transplantation ($p< 0.05$), which consistently increased during the whole testing period when compared with the injured group.

Discussion

In the present study, we demonstrated that rMSC improved functional recovery in rats after SCI. They also reduced the number of apoptotic neurons and oligodendrocytes, and promoted the regeneration or sparing of axons in the injured spinal cord. Degeneration of spinal cord white matter after injury contributes substantially to the pathophysiology of SCI. Even after severe contusive SCI, surviving axons persist in the subpial rim of white matter but exhibit demyelination, which occurs secondary to oligodendroglial cell death, and limited myelin gene expression as well as limited oligodendrocyte renewal after SCI (5,22,26). Also, neurons and oligodendrocytes are highly vulnerable to various insults, and their spontaneous replacement occurs to only a limited extent after damage in the adult spinal cord (27). As treating SCI requires repairing the initial injury of severed fiber tracts as well as fighting widespread secondary damage, stem cell therapy may provide new cells for the regeneration of damaged tissue in the injured areas and new oligodendrocytes for remyelination of injured fiber tracts. Also, through trophic support and extracellular matrix changes, stem cells may counteract factors in the lesioned environment that inhibit axonal regeneration (28). Apart from other types of stem cells, bone marrow stem cells have been studied as candidates for cell replacement therapy as reported previously (29-32). Recently, Cizkova et al., (33) used human mesenchymal stem cells (hMSCs) derived from adult bone marrow. They observed that the transplanted cells were found to infiltrate mainly into the ventrolateral white matter tracts, spreading also to adjacent segments located rostro-caudal to the injury epicenter and further concluded that hMSCs might facilitate recovery from spinal cord injury by remyelinating spared white matter tracts and/or by enhancing axonal growth.

In the present study, we showed transdifferentiation of bone marrow stem cells to neural phenotypes. Since we used the neurogenic medium that promotes differentiation of a mixed culture of neuronal population, trans-differentiation of rMSC to neurons, oligodendrocytes and astrocytes was observed *in vitro*, with neurons being the major population. In contrast, in the injured spinal cord, rMSC differentiated mostly to oligodendrocytes rather than neurons. Since the injured spinal cord will have mostly demyelinated neurons, rMSC probably are more involved in the remyelination of injured fiber tracts. This finding supports the view that transplanted stem cells would ideally replace injured neurons and glial cells by generating new cells (30). These findings are consistent with the previous results (34-38) reporting that stem cells could migrate and accumulate in the injured areas, differentiate into neural cells, and improve the functional recovery of these animals. However, the molecular mechanisms of trans-differentiation of rMSC and their survival *in vivo* for longer periods are being studied.

Similar to our results, apoptotic cell death which predominantly affects oligodendrocytes (6, 8,22,26), has been reported up to three weeks following SCI (8). Decreased apoptosis in rMSC treatments was evident by TUNEL and caspase-3 activation assays. Apoptosis of neurons and oligodendrocytes involves the activation of caspase-3 after traumatic injury to the spinal cord. Our results show that death of injured spinal cord cells in both gray and white matter following moderate spinal cord injury involves processing of caspases-8, -3 and -10 and cleavage of XIAP and PARP, thus contributing probably to the apoptotic death of cells in the spinal cord. In the present study, rMSC attenuates both neuronal and oligodendroglial apoptosis after SCI by down regulating the caspase-3 mediated apoptotic pathway. One of the possible mechanisms by which rMSC down regulate the caspase-3 activation is by inhibiting Fas at the level of plasma membrane. Downregulation of Fas receptor and caspase-3-mediated apoptotic proteins results in improved neurological recovery after SCI, with improved axonal survival and regeneration of neurons and oligodendrocytes. These findings implicate the caspase-3 pathway in apoptotic secondary mechanisms after SCI, particularly in neurons and oligodendrocytes. The effect of downregulation of caspase-3 in preserving mostly oligodendrocytes is consistent with the observation that post-traumatic apoptosis in the spinal cord occurs largely in oligodendrocytes (5,6,14,22,26). In the present investigation, rMSC appear to show the neuroprotective effects to attenuate apoptotic processes by downregulating caspase-3 and other extrinsic pathway proteins during secondary damage of SCI. The anti-caspase-3 activity of rMSC is attributable to downregulation of apoptotic proteins of the extrinsic pathway, which altered the number of caspase-3-positive cells. Similar to our studies, reduction of caspase activity by synthetic peptide-based inhibitors has been demonstrated to attenuate neuronal apoptosis and the spread of secondary damage in animal models of CNS trauma (39,40).

Further, rMSC promoted upregulation of inhibitors FLIP and XIAP in the cytosol and inhibited PARP cleavage in the nucleus. Inhibition of signal transduction by manipulation of molecules such as FLICE (caspase 8) inhibitory protein (FLIP) has not yet been explored. This study provides an evidence that rMSC down regulate caspase-3 extrinsic pathway by increasing the expression of FLIP and XIAP in the cytosol. Activated caspase-3 enzyme contributes to the execution of apoptosis via PARP. This study shows that an up-regulation of PARP after SCI plays an important role in the execution of apoptosis in the injured spinal cord and it can be the potential site for therapeutic intervention after SCI. This is consistent with the previous reports showing that treatment with PARP inhibitors reduces the development of inflammation and tissue injury events associated with spinal cord trauma (41-43). Taken together, rat mesenchymal stem cells used in the present study reduced Fas and activated caspase-3 immunoreactivity in the white matter and grey matter, indicating that these cells can be used to limit the spread of secondary injury. In addition, we found evidence of enhanced neuronal and oligodendrocyte preservation in rMSC-treated rats. There is a significant effect of rMSC in increasing the number of surviving neurons and oligodendrocytes at 14 days after grafting.

In our study, comparing the rMSC-treated animals to the injured rats, we found significant functional recovery after two weeks of rMSC transplantation, improvement in the number of intact axons across the injury site and a decrease in white matter loss. The locomotor recovery of treated rats suggests that the caspase-3 pathway cascade provides a potential therapeutic target in the treatment of SCI. In conclusion, grafted rMSC may contribute to the functional restoration through a combination of regenerating neurons and providing oligodendrocytes for remyelination and inhibit neuronal and oligodendroglial apoptosis through downregulation of caspase-3 pathway cascade. However, successful development of rMSC therapy for spinal cord injury will require a better understanding of the intrinsic properties of these stem cells, the microenvironment, host-graft interactions and subsequently greater functional improvements. Ongoing behavioral and biochemical assessments of the long-term positive effects of rMSC will provide further insight regarding the therapeutic potential of these stem cells for SCI.

Acknowledgements

We thank Noorjehan Ali for technical assistance. We thank Shellee Abraham for manuscript preparation and Diana Meister and Sushma Jasti for manuscript review. This research was supported by National Cancer Institute Grant CA 75557, CA 92393, CA 95058, CA 116708, N.I.N.D.S. NS47699 and NS57529, and Caterpillar, Inc., OSF Saint Francis, Inc., Peoria, IL (to J.S.R.).

References

1. Akiyama Y, Radtke C, Kocsis JD. Remyelination of the rat spinal cord by transplantation of identified bone marrow stromal cells. J Neurosci 2002;22:6623–6630. [PubMed: 12151541]
2. McDonald JW, Liu XZ, Qu Y, Liu S, Mickey SK, Turetsky D, Gottlieb DI, Choi DW. Transplanted embryonic stem cells survive, differentiate and promote recovery in injured rat spinal cord. Nat Med 1999;5:1410–1412. [PubMed: 10581084]
3. Kopen GC, Prockop DJ, Phinney DG. Marrow stromal cells migrate throughout forebrain and cerebellum, and they differentiate into astrocytes after injection into neonatal mouse brains. Proc Natl Acad Sci USA 1999;96:10711–10716. [PubMed: 10485891]
4. Woodbury D, Schwarz EJ, Prockop DJ, Black IB. Adult rat and human bone marrow stromal cells differentiate into neurons. J Neurosci Res 2000;61:364–370. [PubMed: 10931522]
5. Crowe MJ, Bresnahan JC, Shuman SL, Masters JN, Beattie MS. Apoptosis and delayed degeneration after spinal cord injury in rats and monkeys. Nat Med 1997;3:73–76. [PubMed: 8986744]
6. Emery E, Aldana P, Bunge MB, Puckett W, Srinivasan A, Keane RW, Bethea J, Levi AD. Apoptosis after traumatic human spinal cord injury. J Neurosurg 1998;89:911–920. [PubMed: 9833815]
7. Li GL, Farooque M, Holtz A, Olsson Y. Apoptosis of oligodendrocytes occurs for long distances away from the primary injury after compression trauma to rat spinal cord. Acta Neuropathol (Berl) 1999;98:473–480. [PubMed: 10541870]
8. Liu XZ, Xu XM, Hu R, Du C, Zhang SX, McDonald JW, Dong HX, Wu YJ, Fan GS, Jacquin MF, Hsu CY, Choi DW. Neuronal and glial apoptosis after traumatic spinal cord injury. J Neurosci 1997;17:5395–5406. [PubMed: 9204923]
9. Shuman SL, Bresnahan JC, Beattie MS. Apoptosis of microglia and oligodendrocytes after spinal cord contusion in rats. J Neurosci Res 1997;50:798–808. [PubMed: 9418967]
10. Abe Y, Yamamoto T, Sugiyama Y, Watanabe T, Saito N, Kayama H, Kumagai T. Apoptotic cells associated with Wallerian degeneration after experimental spinal cord injury: a possible mechanism of oligodendroglial death. J Neurotrauma 1999;16:945–952. [PubMed: 10547103]
11. Warden P, Bamber NI, Li H, Esposito A, Ahmad KA, Hsu CY, Xu XM. Delayed glial cell death following wallerian degeneration in white matter tracts after spinal cord dorsal column cordotomy in adult rats. Exp Neurol 2001;168:213–224. [PubMed: 11259109]
12. Casha S, Yu WR, Fehlings MG. FAS deficiency reduces apoptosis, spares axons and improves function after spinal cord injury. Exp Neurol 2005;196:390–400. [PubMed: 16202410]
13. Citron BA, Arnold PM, Sebastian C, Qin F, Malladi S, Ameenuddin S, Landis ME, Festoff BW. Rapid upregulation of caspase-3 in rat spinal cord after injury: mRNA, protein, and cellular localization correlates with apoptotic cell death. Exp Neurol 2000;166:213–226. [PubMed: 11085887]
14. Katoh K, Ikata T, Katoh S, Hamada Y, Nakauchi K, Sano T, Niwa M. Induction and its spread of apoptosis in rat spinal cord after mechanical trauma. Neurosci Lett 1996;216:9–12. [PubMed: 8892379]
15. Lee SM, Yune TY, Kim SJ, Park DW, Lee YK, Kim YC, Oh YJ, Markelonis GJ, Oh TH. Minocycline reduces cell death and improves functional recovery after traumatic spinal cord injury in the rat. J Neurotrauma 2003;20:1017–1027. [PubMed: 14588118]
16. Lou J, Lenke LG, Ludwig FJ, O'Brien MF. Apoptosis as a mechanism of neuronal cell death following acute experimental spinal cord injury. Spinal Cord 1998;36:683–690. [PubMed: 9800272]
17. Nottingham S, Knapp P, Springer J. FK506 treatment inhibits caspase-3 activation and promotes oligodendroglial survival following traumatic spinal cord injury. Exp Neurol 2002;177:242–251. [PubMed: 12429226]

18. Nottingham SA, Springer JE. Temporal and spatial distribution of activated caspase-3 after subdural kainic acid infusions in rat spinal cord. J Comp Neurol 2003;464:463–471. [PubMed: 12900917]
19. Springer JE, Azbill RD, Knapp PE. Activation of the caspase-3 apoptotic cascade in traumatic spinal cord injury. Nat Med 1999;5:943–946. [PubMed: 10426320]
20. Springer JE, Azbill RD, Nottingham SA, Kennedy SE. Calcineurin-mediated BAD dephosphorylation activates the caspase-3 apoptotic cascade in traumatic spinal cord injury. J Neurosci 2000;20:7246–7251. [PubMed: 11007881]
21. Yong C, Arnold PM, Zoubine MN, Citron BA, Watanabe I, Berman NE, Festoff BW. Apoptosis in cellular compartments of rat spinal cord after severe contusion injury. J Neurotrauma 1998;15:459–472. [PubMed: 9674550]
22. Casha S, Yu WR, Fehlings MG. Oligodendroglial apoptosis occurs along degenerating axons and is associated with FAS and p75 expression following spinal cord injury in the rat. Neuroscience 2001;103:203–218. [PubMed: 11311801]
23. Basso DM, Beattie MS, Bresnahan JC. A sensitive and reliable locomotor rating scale for open field testing in rats. J Neurotrauma 1995;12:1–21. [PubMed: 7783230]
24. Merkler D, Metz GA, Raineteau O, Dietz V, Schwab ME, Fouad K. Locomotor recovery in spinal cord-injured rats treated with an antibody neutralizing the myelin-associated neurite growth inhibitor Nogo-A. J Neurosci 2001;21:3665–3673. [PubMed: 11331396]
25. Laemmli UK, Favre M. Maturation of the head of bacteriophage T4. I. DNA packaging events. J Mol Biol 1973;80:575–899. [PubMed: 4204102]
26. Li GL, Brodin G, Farooque M, Funa K, Holtz A, Wang WL, Olsson Y. Apoptosis and expression of Bcl-2 after compression trauma to rat spinal cord. J Neuropathol Exp Neurol 1996;55:280–289. [PubMed: 8786386]
27. Ohori Y, Yamamoto S, Nagao M, Sugimori M, Yamamoto N, Nakamura K, Nakafuku M. Growth factor treatment and genetic manipulation stimulate neurogenesis and oligodendrogenesis by endogenous neural progenitors in the injured adult spinal cord. J Neurosci 2006;26:11948–11960. [PubMed: 17108169]
28. Klein S, Svendsen CN. Stem cells in the injured spinal cord: reducing the pain and increasing the gain. Nat Neurosci 2005;8:259–260. [PubMed: 15746908]
29. Ankeny DP, McTigue DM, Jakeman LB. Bone marrow transplants provide tissue protection and directional guidance for axons after contusive spinal cord injury in rats. Exp Neurol 2004;190:17–31. [PubMed: 15473977]
30. Goh EL, Ma D, Ming GL, Song H. Adult neural stem cells and repair of the adult central nervous system. J Hematother Stem Cell Res 2003;12:671–679. [PubMed: 14977476]
31. McDonald JW, Howard MJ. Repairing the damaged spinal cord: a summary of our early success with embryonic stem cell transplantation and remyelination. Prog Brain Res 2002;137:299–309. [PubMed: 12449097]
32. Ruitenberg MJ, Vukovic J, Sarich J, Busfield SJ, Plant GW. Olfactory Ensheathing Cells: Characteristics, Genetic Engineering, and Therapeutic Potential. J Neurotrauma 2006;23:468–478. [PubMed: 16629630]
33. Cizkova D, Rosocha J, Vanicky I, Jergova S, Cizek M. Transplants of human mesenchymal stem cells improve functional recovery after spinal cord injury in the rat. Cell Mol Neurobiol 2006;26:1167–1180. [PubMed: 16897366]
34. Kuh SU, Cho YE, Yoon DH, Kim KN, Ha Y. Functional recovery after human umbilical cord blood cells transplantation with brain-derived neutrophic factor into the spinal cord injured rat. Acta Neurochir (Wien) 2005;147:985–992. [PubMed: 16010451]
35. Liu S, Qu Y, Stewart TJ, Howard MJ, Chakrabortty S, Holekamp TF, McDonald JW. Embryonic stem cells differentiate into oligodendrocytes and myelinate in culture and after spinal cord transplantation. Proc Natl Acad Sci USA 2000;97:6126–6131. [PubMed: 10823956]
36. Lu P, Jones LL, Tuszynski MH. BDNF-expressing marrow stromal cells support extensive axonal growth at sites of spinal cord injury. Exp Neurol 2005;191:344–360. [PubMed: 15649491]
37. Lu P, Jones LL, Snyder EY, Tuszynski MH. Neural stem cells constitutively secrete neurotrophic factors and promote extensive host axonal growth after spinal cord injury. Exp Neurol 2003;181:115–129. [PubMed: 12781986]

38. Saporta S, Kim JJ, Willing AE, Fu ES, Davis CD, Sanberg PR. Human umbilical cord blood stem cells infusion in spinal cord injury: engraftment and beneficial influence on behavior. J Hematother Stem Cell Res 2003;12:271–278. [PubMed: 12857368]

39. Movsesyan VA, Yakovlev AG, Fan L, Faden AI. Effect of serine protease inhibitors on posttraumatic brain injury and neuronal apoptosis. Exp Neurol 2001;167:366–375. [PubMed: 11161625]

40. Ozawa H, Keane RW, Marcillo AE, Diaz PH, Dietrich WD. Therapeutic strategies targeting caspase inhibition following spinal cord injury in rats. Exp Neurol 2002;177:306–313. [PubMed: 12429232]

41. Genovese T, Mazzon E, Di Paola R, Muia C, Threadgill MD, Caputi AP, Thiemermann C, Cuzzocrea S. Inhibitors of poly(ADP-ribose) polymerase modulate signal transduction pathways and the development of bleomycin-induced lung injury. J Pharmacol Exp Ther 2005;313:529–538. [PubMed: 15644425]

42. Keane RW, Kraydieh S, Lotocki G, Bethea JR, Krajewski S, Reed JC, Dietrich WD. Apoptotic and anti-apoptotic mechanisms following spinal cord injury. J Neuropathol Exp Neurol 2001;60:422–429. [PubMed: 11379817]

43. Scott GS, Szabo C, Hooper DC. Poly(ADP-ribose) polymerase activity contributes to peroxynitrite-induced spinal cord neuronal cell death *in vitro*. J Neurotrauma 2004;21:1255–1263. [PubMed: 15453994]

Abbreviations

APC
Adenomatous polyposis coli

BBB
Basso Beattie Bresnahan locomotor scoring

BCA
Bicinchoninic acid

BDNF
Brain derived neurotrophic factor

bFGF
basic fibroblast growth factor

BSA
Bovine serum albumin

CHAPS
3-[(3-Cholamidopropyl) dimethylammonio]-1-propanesulfonate

CNPase
2′, 3’-cyclicnucleotide-3′-phosphodiesterase

DAB
Diaminobenzidine

DAPI
4′, 6-Diamidino-2-phenylindole dihydrochloride

DPI
days post injury

DTT
Dithiothreitol

FBS

Fetal bovine serum

FITC
Fluorescein isothiocyanate

FLIP
FLICE-inhibitory protein

GFAP
Glial fibrillary acidic protein

hEGF
human epidermal growth factor

HRP
Horseradish peroxidase

β-NGF
Beta-nerve growth factor

NF-200
Neurofilament H-200 kD

NT-3
Neurotrophic hormone-3

PARP
poly [ADP- ribose] polymerase

PBS
Phosphate buffered saline

PMSF
Phenyl methane sulfonyl fluoride

RA
Retinoic acid

rMSC
Rat bone marrow mesenchymal stem cells

SCI
Spinal cord injury

XIAP
X-linked inhibitor of apoptosis protein

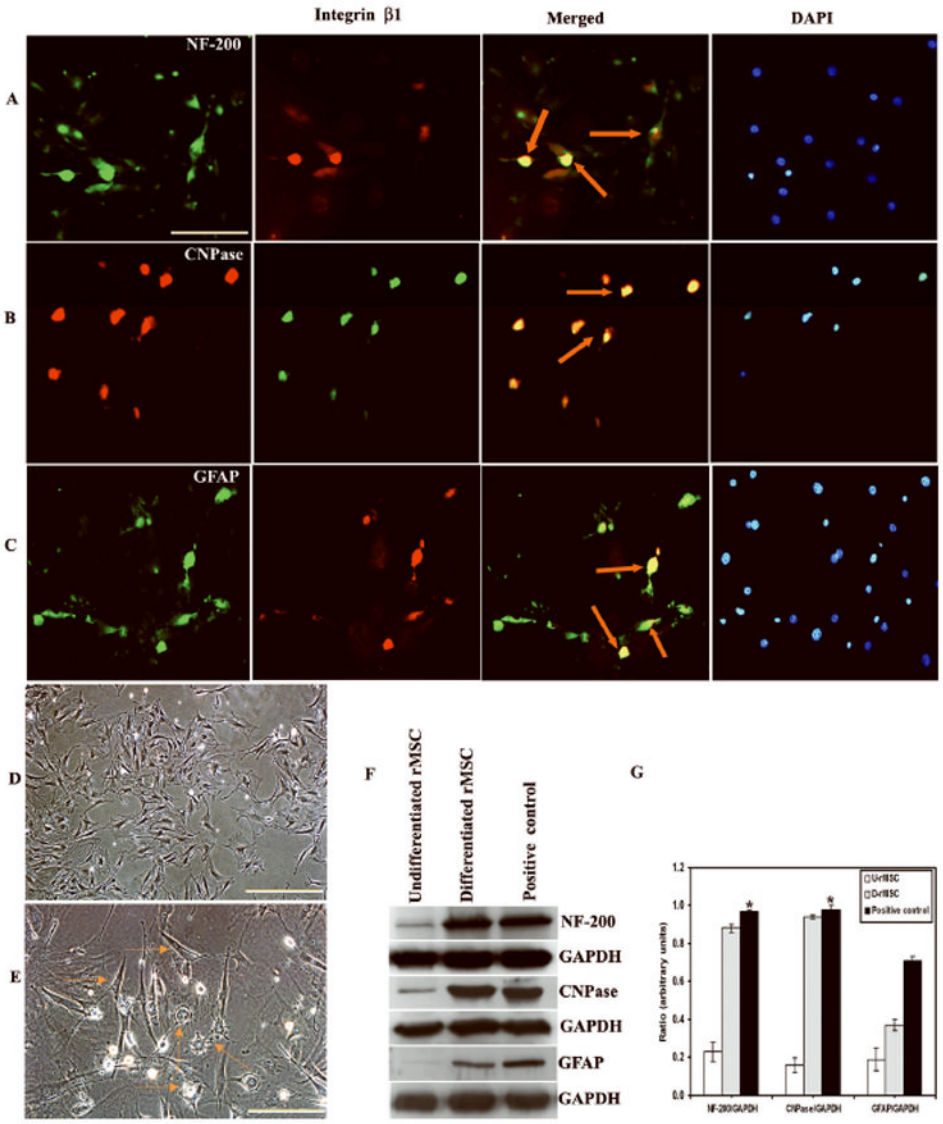

Fig. 1. ***In vitro*** **differentiation of rMSC into neural phenotypes**

Photomicrographs of rMSC in mixed culture demonstrating neural proteins expressed by the cells before transplantation. Dual staining of (A) Texas-red conjugated -Integrin β1 (for rMSC) with FITC-conjugated-NF-200, (B) Texas-red conjugated CNPase (for oligodendrocytes) with FITC-conjugated Integrin β1(for rMSC) and (C) Texas-red conjugated -Integrin β1 (for rMSC) with FITC-conjugated-GFAP (for astrocytes) demonstrates that rMSC in neural induction medium differentiate into respective neural phenotypes. (D) Phase-contrast image of undifferentiated rMSC. (E) Phase-contrast image of differentiating rMSC after three days showing mixed population of neural phenotypes. (F) Western blot showing neural proteins in differentiated population. Equal amounts of protein (40 μg) were loaded onto 10%-14% gels and transferred onto nylon membranes, which were then probed with respective antibodies. The blots were stripped and reprobed with GAPDH to assess protein levels. (G) Quantitative estimation of neural proteins in Fig. F. (U- rMSC = Undifferentiated rMSC; D- rMSC = Differentiated rMSC; Positive control = Whole brain extract of rat). The results are from nine independent cultures (three parallel experiments from three separate passages of rMSC). A subpopulation of rMSC-derived cells growing in a monolayer before clone formation was

found to be negative for all investigated antigens. Merged figures include phase-contrast and co-localized markers. For panels A, B and C, Bar = 100 μm. For panels D and E, Bar = 200 μm. (Error bars indicate SEM. * Significant at $p < 0.05$).

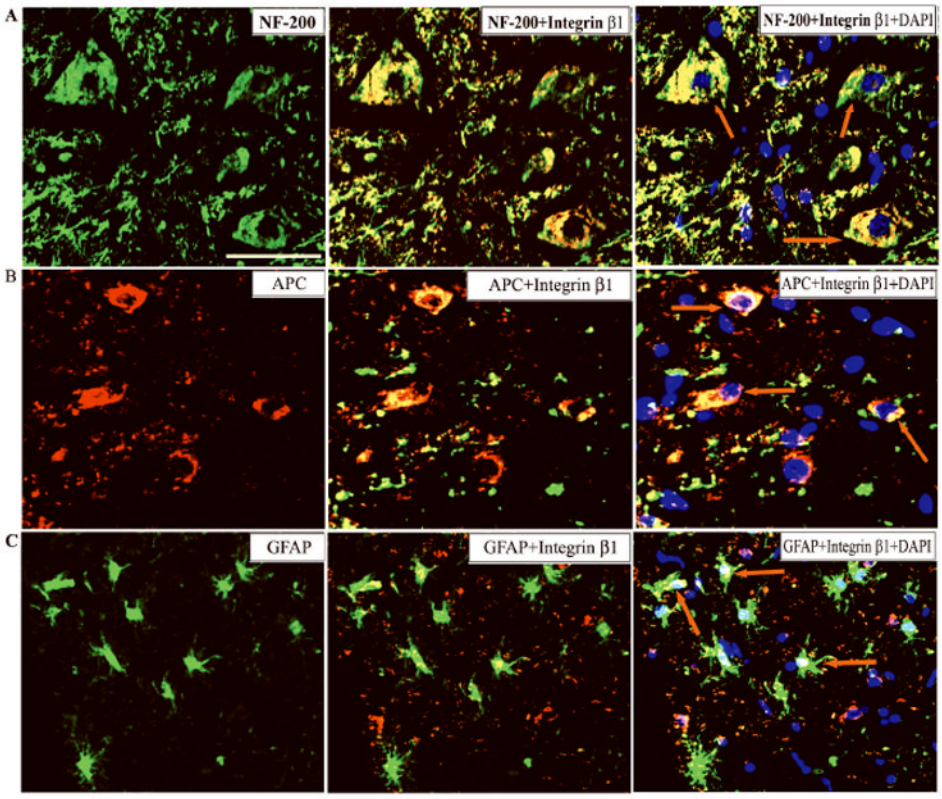

Fig. 2. Transplanted rMSC differentiate into neurons, oligodendrocytes and astrocytes *in vivo* after SCI

Confocal immunohistochemistry on longitudinal sections of the injured spinal cords of rats 5 weeks after transplantation is shown. 7 days after spinal cord injury, the rMSC -transplanted group received a 5 μL mononuclear cell layer of rMSC cells (5×10^5 cells/μL). Immunofluorescence analysis of cryo-sections indicates co-localization (yellow) of (A) FITC-conjugated NF-200 (a marker of neurons) with rMSC (Texas-red conjugated-Integrin β1) and DAPI, (B) rMSC (FITC conjugated-Integrin β1) with Texas-red conjugated -APC (a marker of mature oligodendrocytes) and (C) FITC-conjugated GFAP (a marker of astrocytes) with rMSC (Texas-red conjugated Integrin β1) following transplantation into the injured spinal cords, shown by (↑). The tissue sections represent dorsal regions 2 mm from the lesion epicenter ($n \geq 3$). The results are from three independent sections between 1 and 2mm from the injury epicenter from treated rats in each group (n=3). Bar = 100 μm.

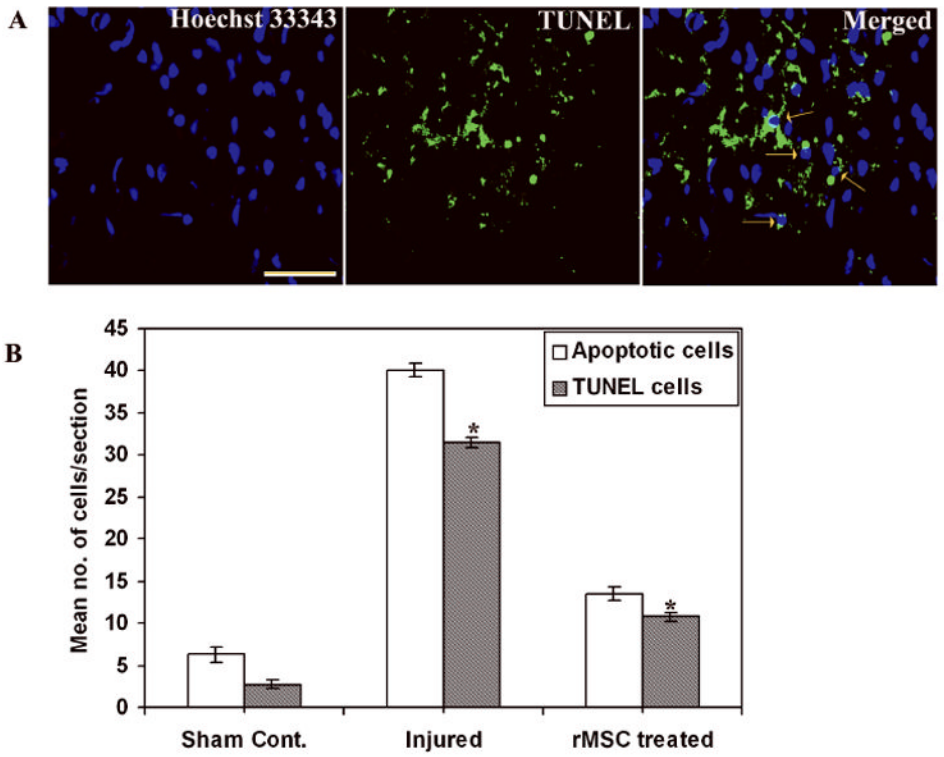

Fig. 3. Expression of apoptotic and TUNEL cells in spinal cord sections of rats

(A) Cryo-sections from injured rats after 3 weeks stained with Hoechst 33343 shows apoptotic cells with bright fluorescence, TUNEL stained sections showing TUNEL-positive cells and merged image showing TUNEL cells on apoptotic cells (↑). Bar = 100 μm. (B) Quantitative estimation of apoptotic and TUNEL cells. (Error bars indicate SEM. * Significant at $p < 0.05$). Results are from three independent sections between 1 and 2 mm from the injury epicenter (n = 3).

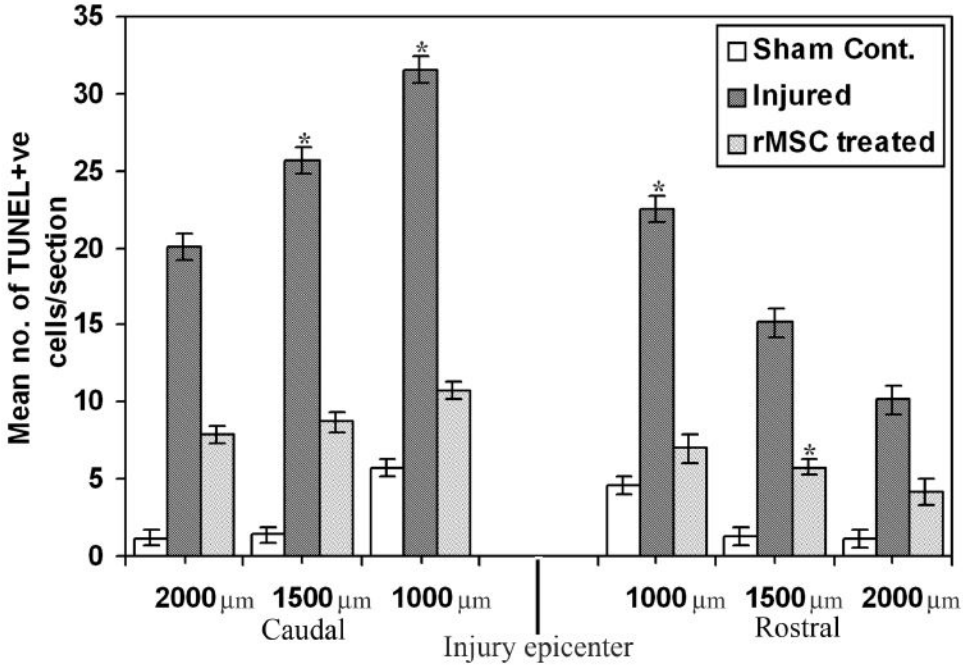

Fig. 4.

Quantitative estimation of apoptotic and TUNEL-positive cells in the tissue sections up to 2 mm rostral and caudal to the injury epicenter. (Error bars indicate SEM. * Significant at $p < 0.05$). Results are from three independent sections between 1 and 2 mm from the injury epicenter (n = 3).

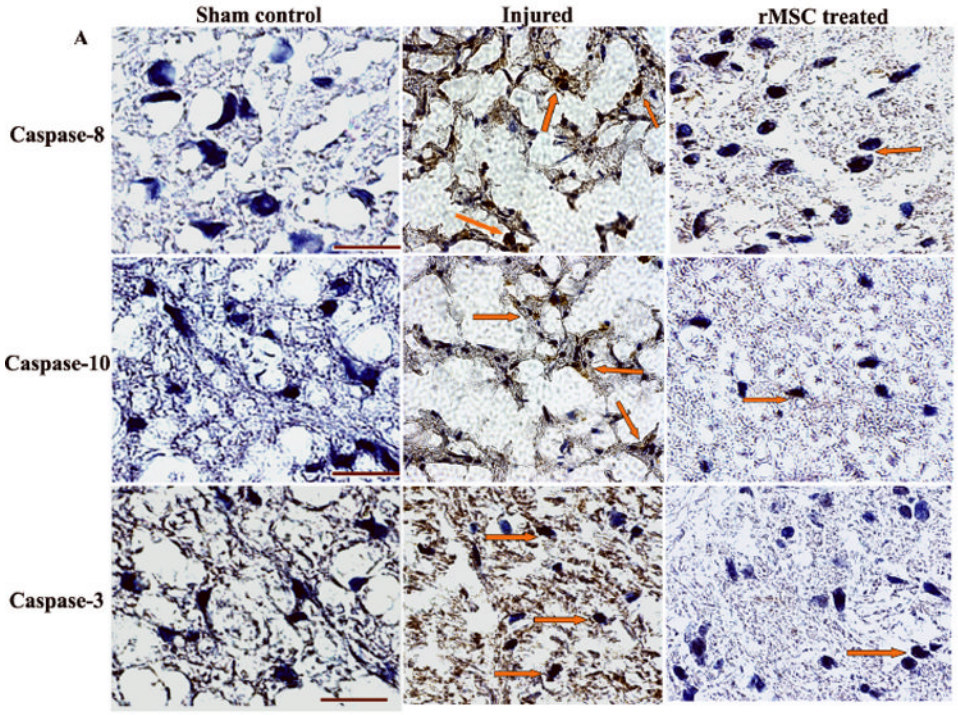

Fig. 5. Expression of caspases after spinal cord injury

To evaluate the expression of caspases after SCI, we used diamino benzidine (DAB) immunostaining with antibodies for caspases 8, 10 and 3. The sections are counter stained with hematoxylin for nuclear localization. Notably, the immunoreactivity is much higher in the injured sections than in the treated sections (↑). Results are from three independent sections between 1 and 2 mm from the injury epicenter (n = 3). Bar = 100 μm.

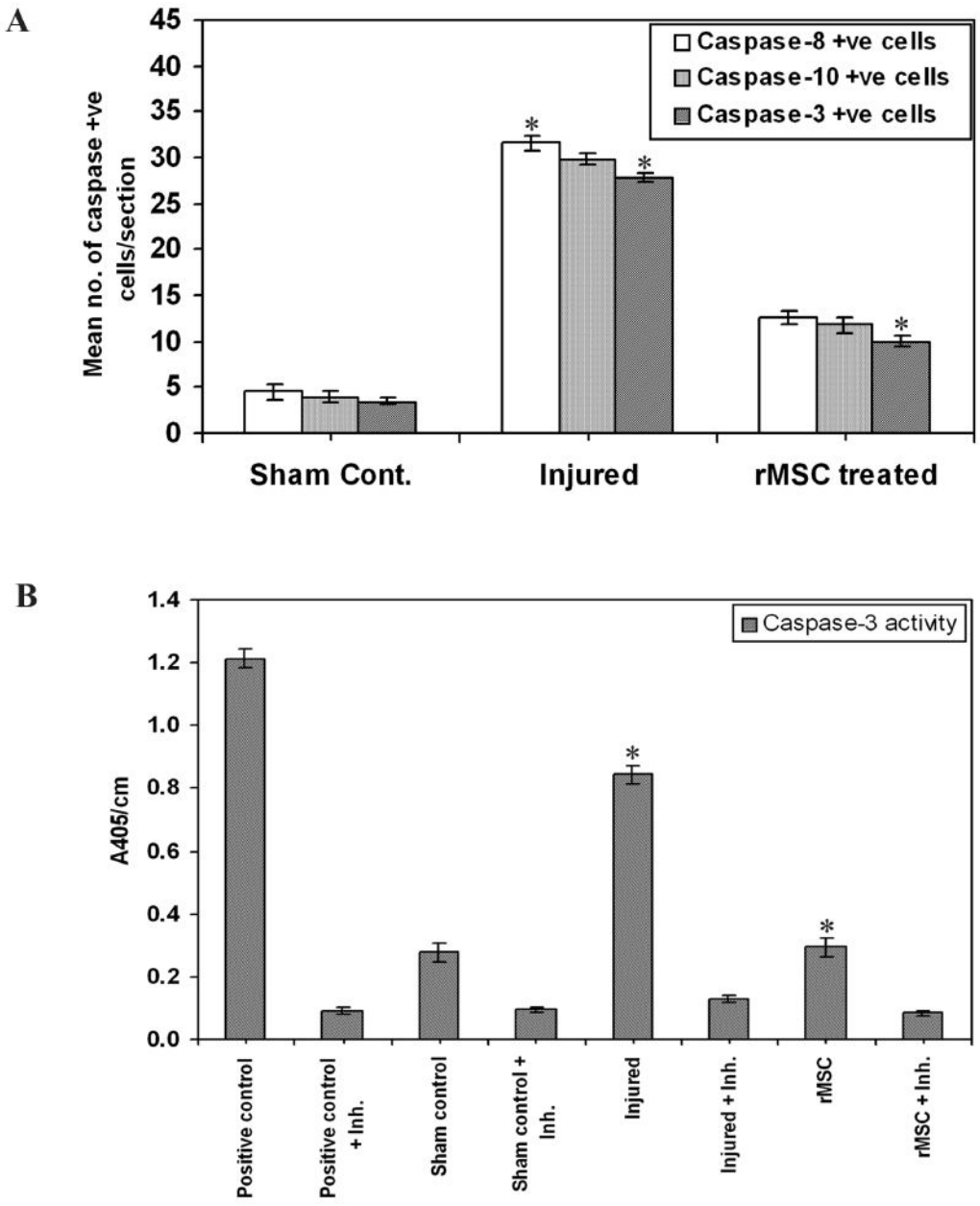

Fig. 6. Caspase-3 activity in injured spinal cords

(A) Quantitative estimation of the number of caspase-positive cells in each section. Results are from three independent sections between 1 and 2mm caudal to the injury epicenter (n = 3). (B) Caspase-3 enzyme activity was assayed in tissue lysates of spinal cord. Equal amounts of protein (50 μg) were assayed for caspase-3 activity for 30 min in an ELISA plate reader, measuring absorption at 405 nm. Purified caspase-3 enzyme was used as a positive control. The injured tissues show maximum enzymatic activity when compared to the treated tissues, which show activity similar to that of the control groups. Inh. = Ac-DEVD-CHO inhibitor. (Error bars indicate SEM. * Significant at $p < 0.05$). The experiment is repeated twice with triplicates (n = 3).

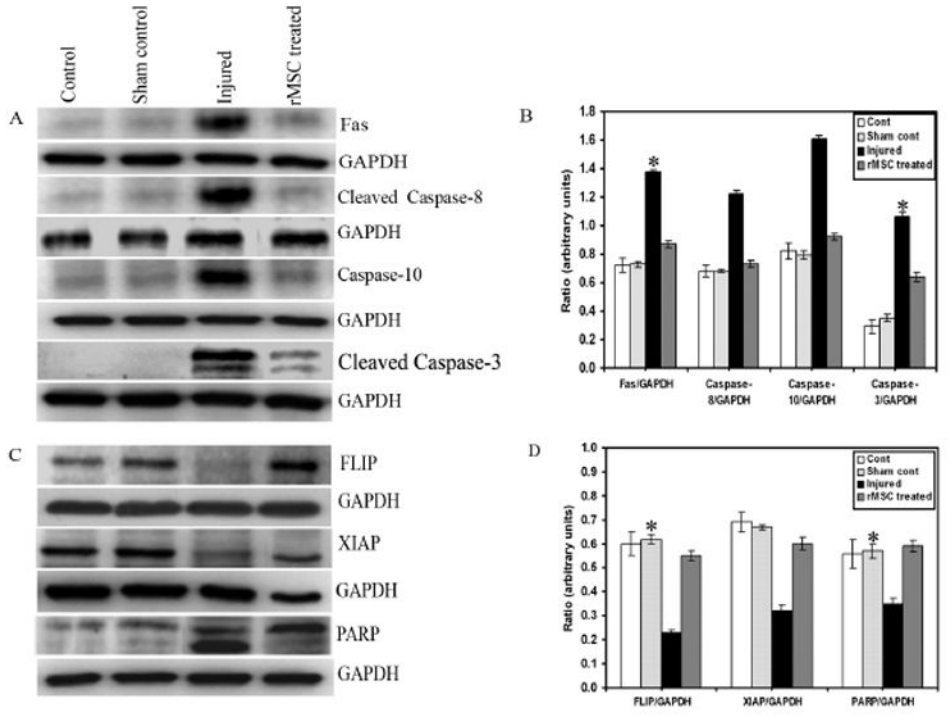

Fig. 7. Immunoblot analysis of caspase-3-mediated apoptotic pathway in spinal cord sections

Equal amounts of protein (40 μg) were loaded onto 10%-14% gels and transferred onto nylon membranes, which were then probed with respective antibodies. The blots were stripped and reprobed with GAPDH to assess protein levels. A and C shows the Fas and caspase-3 mediated apoptotic pathway proteins with respect to GAPDH; B and D are their quantitative estimations, respectively. Inhibition of the caspase-3-mediated apoptotic pathway by rMSC shows downregulation of Fas and caspases, upregulation of FLIP, XIAP, and inhibition of PARP cleavage. Antisera for caspase-8 and caspase-3 recognize cleaved fragments also. Each blot is representative of experiments performed in duplicate with each sample (n = 3). Error bars indicate SEM. * Significant at $p < 0.05$.

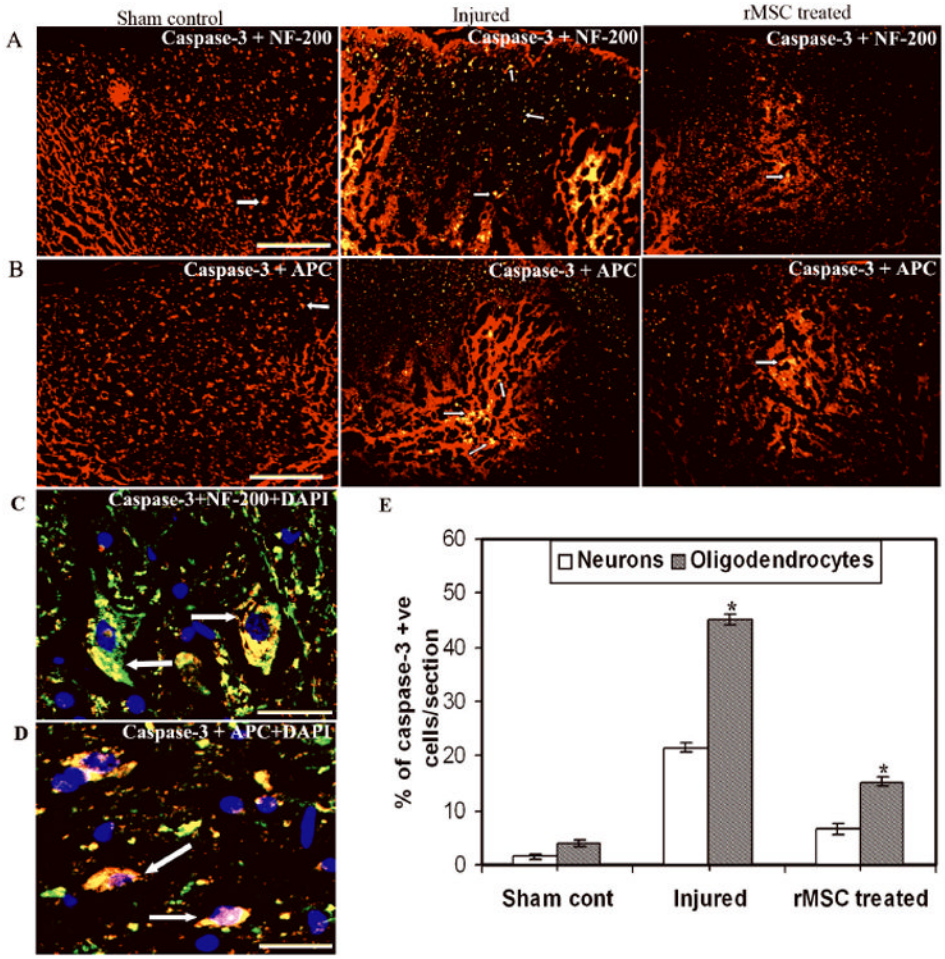

Fig. 8. Immunofluorescence analysis of caspase-3 expression in neurons and oligodendrocytes

Photomicrographs illustrate co-localization (yellow) of activated caspase-3 (FITC-conjugated) with (A) NF-200 (Texas-red conjugated) and (B) with APC (Texas-red conjugated) in the dorsal white matter and grey matter (↑), following spinal cord contusion. The tissue sections represent regions between 1 and 2 mm caudal from the lesion epicenter. A and B showing the injured area at low magnification. C and D showing expression of caspase-3 on neurons and oligodendrocytes respectively, at higher magnification. For panels A and B, Bar = 200 μm. For panels C and D, Bar = 100 μm. (E) Quantitation of apoptotic neurons and oligodendrocytes in tissue sections. Values represent mean ± SEM values of at least three sections with duplicates from each condition. * Significant at $p < 0.05$. A large number of caspase-3 positive cells are present in the injured sections, whereas the rMSC-treated sections exhibit a decreasing trend of caspase-3 positive cells. Results are from three independent sections between 1 and 2 mm from the injury epicenter (n = 3).

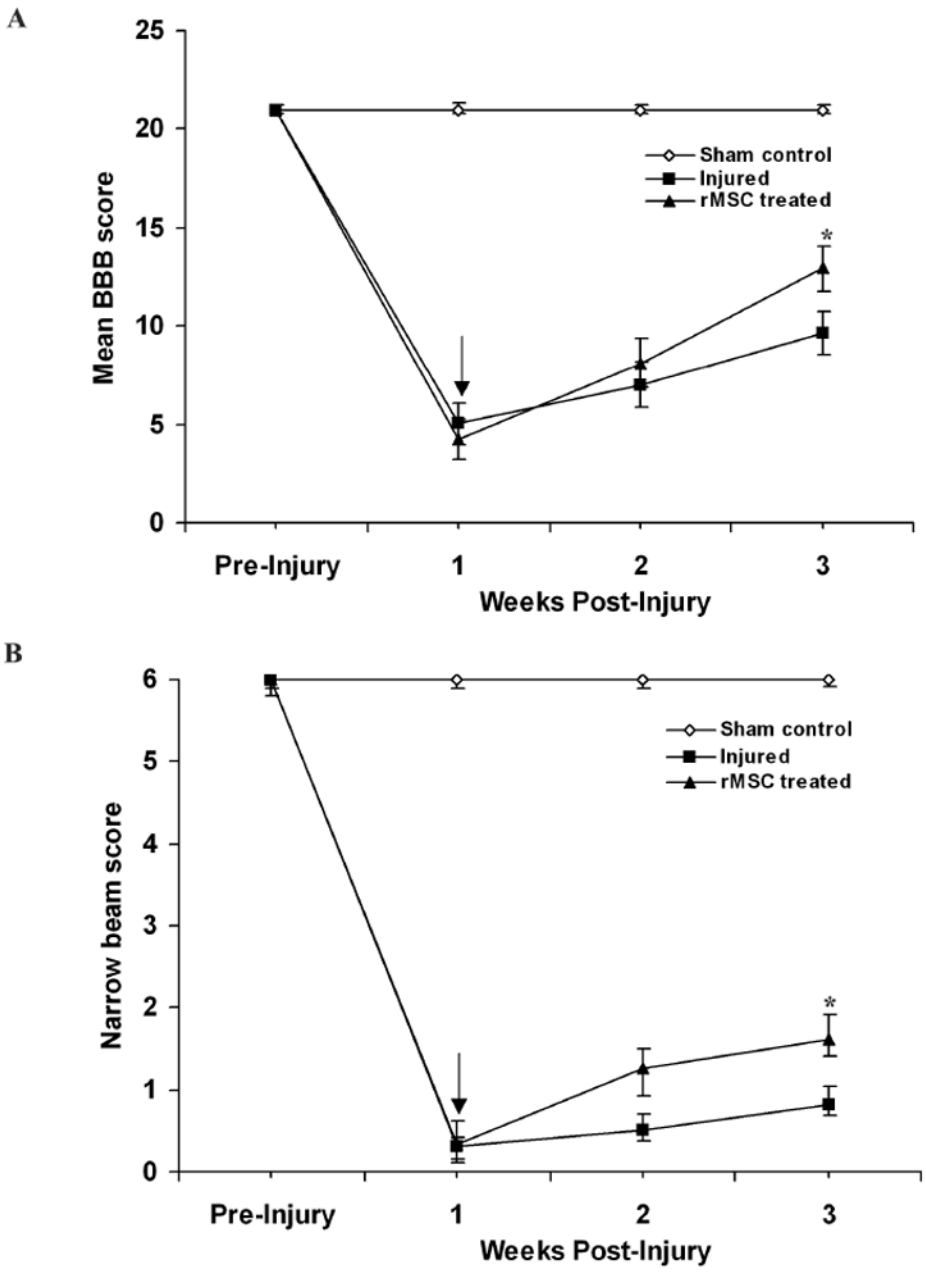

Fig. 9. Functional recovery of rats after rMSC treatments

(A) BBB scores of rats with SCI before and after rMSC transplantation at 7 days post SCI indicate that rMSC transplantation significantly improved hindlimb performance in both hind legs. Repeated-measures of ANOVA followed by Bonferroni's post hoc tests showed that BBB scores in rMSC -grafted animals were significantly higher than those in injured-untreated animals (*p<0.05). Each point represents the highest locomotor score achieved each day. (B) Time course of the recovery in rMSC-treated rats in the narrow-beam test. The ability of the rats to walk on differently shaped wooden beams is scored from 0 to 6 (see Methods). Arrow (↓) indicates transplantation point. Error bars indicate SEM (n>5 per group).